Published by
NIGERIAN SOCIETY OF PHYSICAL SCIENCES
Available online @ https://journal.nsps.org.ng/index.php/jnsps

J. Nig. Soc. Phys. Sci. 7 (2025) 2429

Journal of the Nigerian Society of Physical Sciences

Quantitative reservoir evaluation and hydrocarbon volumetrics: an integrated petrophysical and 3-D static modeling approach in 'Hamphidex' field, Niger-Delta, Nigeria

Akindeji Opeyemi Fajana[a,*], Adam Muhammed Olawale[a], Hammed Ajibola Oyesomi[b]

[a]*Department of Geophysics, Federal University Oye-Ekiti, Nigeria*
[b]*Halliburton Energy Services Limited, Lagos, Nigeria*

Abstract

The viability and hydrocarbon volumetrics of the Hamphidex field reservoirs were evaluated using petrophysical analysis and three-dimensional (3D) static modeling of three key reservoir sands (X, Y, and Z). The petrophysical analysis involved detailed characterization of lithologies, net-to-gross ratios, porosity, hydrocarbon saturation, water saturation, and permeability. The volumetric attributes of the field were derived from the constructed 3D reservoir models. Two geostatistical methods–Sequential Gaussian Simulation (SGS) and Sequential Indicator Simulation (SIS)–were utilized for facies and property modeling, focusing on porosity and permeability. Comprehensive facies models and petrophysical property models were developed for each reservoir sand (X, Y, and Z), integrating 3D visualizations of facies distributions, porosity, permeability, water saturation, and fluid contact models. Two main facies, sand and shale, were identified, with sand acting as the hydrocarbon reservoir. Well-log correlations in six wells (Hamdex-02, 06, 01, 05, 04 and 07) of the field show that sands X, Y, and Z have lateral continuity and their hydrocarbon potential varies between wells. Specifically, Sand 'X' contains hydrocarbons in Hamdex-05 and Hamdex-07, Sand 'Y' is hydrocarbon-rich in Hamdex-05, and Sand 'Z' shows hydrocarbon presence in Hamdex-06, Hamdex-05, and Hamdex-04. For Sand X, Y, and Z, porosity values range between 16 and 25%, permeability varies from 10 to 1600 mD, water saturation lies within 7 to 50%, and hydrocarbon saturation spans from 50 to 93%. The volumetric assessments from the build models showed that Sand X, Y and Z have Stock-Tank-Oil-Initially-In-Place (STOIIP) of 75.864, 8.566 and 80.177 Million Barrels (MMbbl), respectively. In addition to Sand Y STOIIP it also has Gas-Initially-In-Place (GIIP) of 14.870 Billion Standard Cubic Feet (Bscf). These findings demonstrate that the field is economically viable and suitable for development, presenting a strong potential for successful exploitation.

DOI:10.46481/jnsps.2025.2429

Keywords: Lithologies, Net-to-gross, Hydrocarbon saturation, Hydrocarbon reserves

Article History :
Received: 10 October 2024
Received in revised form: 28 November 2024
Accepted for publication: 10 December 2024
Available online: 13 January 2025

Communicated by: O. J. Abimbola

1. Introduction

1.1. Background of the study

Revenue generated from crude oil constitutes a significant portion of Nigeria's Gross Domestic Product (GDP). Consequently, there is a continuous drive to identify additional hydrocarbon reserves of commercial value from both existing and untapped fields. Beyond crude oil sales, the Nigerian government derives revenue in the upstream oil sector through mechanisms such as leasing or licensing oil fields to bidders, as well as taxes and royalties on produced oil [1]. Before granting an Oil Prospecting License (OPL) or Oil Mining Lease (OML),

*Corresponding author: Tel.: +234-803-825-9701.
Email address: akindeji.fajana@fuoye.edu.ng (Akindeji Opeyemi Fajana)

the government, typically through its geoscientists, assesses the viability of an oil field by estimating the Hydrocarbon Initially in Place (HCIIP). This evaluation is critical for both the government and prospective bidders. While the government seeks to ascertain the field's potential value, bidders aim to determine whether the field is a profitable asset or a potential liability before and after acquisition, particularly during the bidding process.

This field(s) assessment is done by using the sparse well log data each showing a point drilled and 3-D seismic data. An in-depth assessment is done by building a 3-D Static reservoir Model that predicts possible details of the point where the wells are situated and other areas away from the well in a particular reservoir(s) in a field [2, 3]. The estimate of possible volumes of the field's hydrocarbon which coupled with other factors, form the limits (minimum bar) criteria for the acquisition and development of such field. The determination of a field's subsurface reservoir rock petrophysical properties such as porosity, permeability, water saturation, and the area extent from well log data and the built model usually gives insight into a field's reservoir quality in which the sort after petroleum is stored [4–6]. The Three-Dimensional Static reservoir modelling is usually an attempt to describe the subsurface reservoir of a particular field as it is (in situ) at a particular time [7]. The resulting outcome of petrophysics and interpreted 3-D seismic forms the basis for the development of suitable facie and property models of a 3-D static model.

A suitably developed 3-D static reservoir model is usually a representative geologic model of discrete properties (facies) and dynamic properties (petrophysical) generated from various data interpretations on Earth Modelling Software and it enables experienced interpreters to have a true picture and garnered knowledge of the subsurface similar to the physical visualization of the subsurface reservoir rock in a 3-Dimensional form. This efficient knowledge of the abstract subsurface is transformed to guide the development of a field reservoir. It also helps improve the hydrocarbon recovery rate because a low recovery rate usually arises from an inefficient sweep of the reservoir caused by poor inter-well-scale heterogeneities knowledge.

These 3-D static reservoir model parameters are usually required for the calculation of possible hydrocarbon volumetric inside the reservoir and also in the development of Dynamic Reservoir Models whereby a simulation model predicting the possible movement of hydrocarbon in reservoir rock is done.

Also, these realistic 3-D geological model when used judiciously, in turn, leads to devising a better strategy, planning, deciding and executing in the best way the production of hydrocarbon in commercial quantity from a field [8]. Hence, reservoir modelling is the main area of current hot topics in reservoir geoscience.

1.2. Location and geomorphology of the study area

The study was conducted on the "Hamphidex" field located in Niger-Delta, Nigeria (Figure 1). This field covered latitude 65000 to 73200 Nm and longitude 477000 to 485000 Em and it is about 55.83 (sq. km) which is about 13,796 acres as shown in the base map (Figure 2). The study area experiences

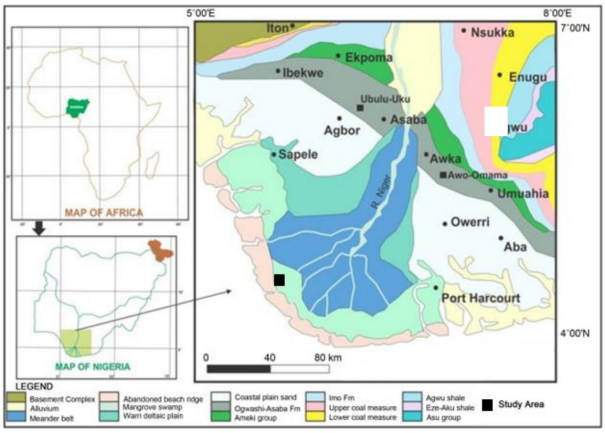

Figure 1: Map of Niger-Delta and its surroundings [9].

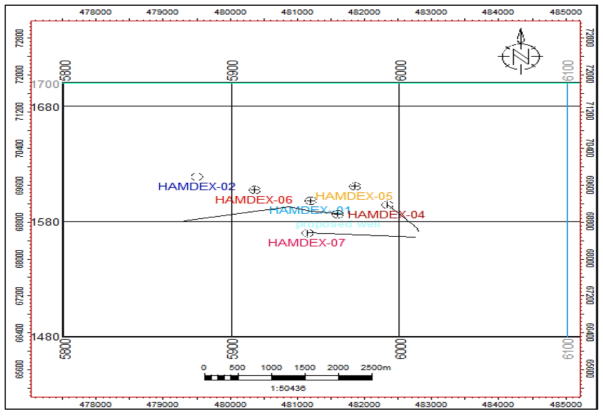

Figure 2: Base map of Hamphidex field.

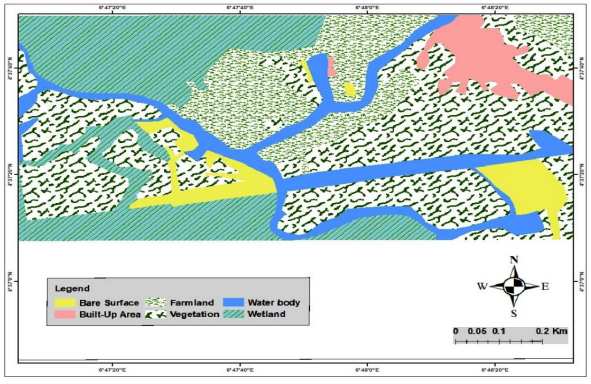

Figure 3: Satellite imagery showing details of the Study Area [10].

a monsoonal climate with two distinct seasons: the dry season (November to April), characterized by harmattan winds, and the rainy season (May to October), occasionally interrupted by a drier spell in August [11]. Rainfall can occur even during the dry season. The region's vegetation is predominantly rainforest, transitioning to swamplands in some areas, with diverse flora including timber, palm, and fruit trees. A satellite imagery map of the area is presented in Figure 3.

2. Geology of the study area

The geology of the "Hamphidex" field aligns with that of a tropical delta located on the passive continental margin of the South Atlantic, consistent with the broader geological framework of the Niger Delta. The field's stratigraphy dates from the Early Tertiary to the Recent period, and it is characterized by a shallow ramp depositional model. Data from the wells in the field indicate that the reservoirs consist predominantly of sands and interbedded sand-shale sequences, typical of the Agbada Formation (also referred to as the Ogwashi-Asaba Formation). These reservoirs are classified as deltaic sandstones and stacked sand-shale alternations, a hallmark of the Niger Delta geology [12]. The Agbada Formation, of Eocene age, directly overlies the Akata Formation and serves as the primary hydrocarbon-bearing unit. Reservoir depths within the Niger Delta, including the "Hamphidex" field, are observed to range between 5,000 and 14,000 feet, highlighting the substantial vertical extent of the productive intervals. This stratigraphic and depositional context underscores the field's geological suitability for hydrocarbon exploration and production. The Akata Formation which is known to be the Source rock in the Niger Delta has been dated to be Paleocene in age. It is composed of Marine shale rich in Land plant material buried in an anaerobic environment. The Marine planktonic foraminifera make up to 50% of the microfauna assemblage. The absence of oxygen was due to the depth of burial of these plants that decay to form Kerogen from which the Hydrocarbon is formed. The Akata Formation top oil window is known to be about 9000 to 14000 ft with a known temperature of about 240° F (115°C) and its base has not been determined [13].

The Benin Formation is the formation overlying the Agbada Formation. It is known to be Oligocene and younger and composed of continental floodplain sands and alluvial deposits. It has been determined to be about 2000 m thick. The Formations are shown in Figure 4.

Traps in the field are structural, they include Anticlines and Faults. They are typical of Niger Delta whose traps are known to include Dip Closures, Fault bound traps and stratigraphic traps (Figure 5). In trap configuration, growth faults and antithetic faults are crucial. Growth faults have a large throw (up to several hundred metres), are arcuate, concave basinward, and can extend for several tens of kilometres. The throw of an antithetic fault is often less than one hundred metres. They rarely surpass ten kilometres in length and can be either linear or arcuate in plain view.

Hydrocarbons in the Niger Delta region include oil or condensates and gas with gravity between 15 to 25 API for the biodegraded. The non-biodegraded has gravity between 25 to 45 API. It is low in sulphur/nickel to pristane/phytane ratio is 0.6 to 1.6. It is also rich in resin [14].

2.1. Materials used for the study

The materials used for this study include a base map representing the study area, which covers approximately 13,796 acres (˜55.83 km^2) and displays seismic lines (in-lines and cross-lines) along with the relative positions of six wells. These

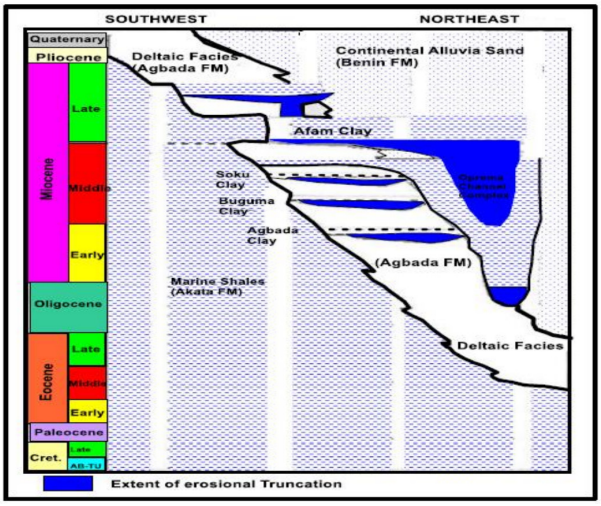

Figure 4: Typical stratigraphic layers of the Niger Delta. (Carved out from Ref. [15]).

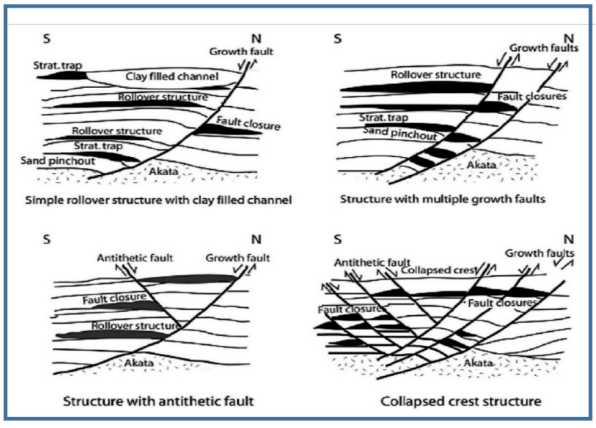

Figure 5: Common structures and traps delineated in oil fields in Niger Delta (Carved out from Ref. [12]).

wells, namely Hamdex-02, Hamdex-06, Hamdex-01, Hamdex-05, Hamdex-04, and Hamdex-07, provided well log data such as gamma-ray (GR), resistivity (IDL), density (RHOB), neutron (NPHI), and sonic logs, essential for lithological and reservoir characterization. Check-shot data, measuring travel times from surface shotpoints to geophones at known well depths, were employed for time-to-depth conversion, aligning seismic data (in time) with well data (in depth). These data, along with sonic and density logs, were used to generate synthetic seismograms and enhance depth conversion, facilitating well-to-seismic ties. Additionally, a post-stack 3D seismic volume comprising 400 in-lines, 220 cross-lines, and time slices was analyzed. For instance, seismic in-line 6000, cross-line 1700, and time slice 2100 were key references, with the data characterized by positive American polarity (blue as peaks and red as troughs) and exhibiting varied reflection geometries from high to low amplitudes, as illustrated in Figure 6. These materials collectively provided a comprehensive dataset for the study's analysis and interpretation.

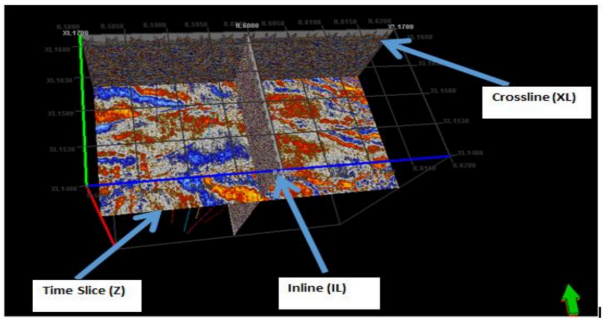

Figure 6: Typical in-lines (6000) and cross-line XL (1700) and time slice Z (2100).

2.2. Methods used for the study

The study's methodology involved loading and preparing data for analysis using Petrel software, where data stored in standard formats were imported into the workspace, rescaled, and quality-checked for further interpretation. The petrophysical analysis began with qualitative log interpretation to identify trends, lithology, fluid types, and contacts. Lithology was determined using a gamma-ray log, with a cutoff value of 70 API units distinguishing shale (above 70 API) from sand (below 70 API). Reservoir delineation utilized gamma-ray and deep-resistivity logs, where low gamma-ray and high resistivity responses signified hydrocarbon reservoirs. To resolve ambiguities, neutron and density logs were integrated, confirming fluid types and providing precise reservoir characterization. Fluid contacts were identified by analyzing log responses across gas, oil, and water zones, using density, neutron, and resistivity logs. For gas zones, low density and neutron readings paired with high resistivity indicated gas presence, while oil zones showed increased density and neutron log responses with sustained high resistivity. Water-bearing zones were identified by reduced resistivity due to salinity.

Well log correlation across six wells in the "Hamdex" field established lateral continuity and stratigraphic equivalence. Shale layers, owing to their widespread distribution and consistency, were used as reference datums for correlation. This facilitated the identification of continuous and discontinuous sand layers, delineating their tops and bases to refine the understanding of the lithological and stratigraphical framework.

2.3. Quantitative log interpretation

2.3.1. Gross thickness

It was calculated by deducting the reservoir's top depth value from the reservoir's base depth value. According to Ref. [9]:

$$\text{Gross thickness} = \text{Base of reservoir} - \text{Top of reservoir}. \quad (1)$$

2.3.2. Net thickness

This parameter was determined by subtracting shale intervals from the gross thickness. According to Ref. [9]:

$$\text{Net thickness} = \text{Gross thickness} - \text{Shale intervals thickness}. \quad (2)$$

2.3.3. Net to gross thickness

It was calculated using equation (3). According to Ref. [9]:

$$NTG = \frac{\text{Net thickness}}{\text{Gross thickness}}. \quad (3)$$

2.3.4. Volume of shale

This parameter was calculated using the gamma-ray log. According to Ref. [9],

$$I_{\text{GR}} = \frac{(\text{GR}_{\text{log}} - \text{GR}_{\text{min}})}{(GR_{\text{max}} - \text{GR}_{\text{min}})}, \quad (4)$$

where I_{GR} represents gamma-ray-index, GR_{log} denotes gamma-ray response across reservoir interval, GR_{max} denotes gamma-ray response across shale, GR_{min} indicates gamma ray minimum response across the sand, Larionov formula (equation (5)) was used for the final volume of shale computation.

$$V_{\text{sh}} = 0.083 \times (2^{3.7 \times I_{\text{GR}}} - 1.0). \quad (5)$$

The equation (5) was specifically chosen because it applies to Tertiary rocks and the Niger Delta basin age falls in that category.

2.3.5. Porosity

According to Ref. [9], the Porosity is computed

$$\Phi_{\text{Density}} = \frac{\rho_{\text{ma}} - \rho_b}{\rho_{ma-\rho_{\text{fl}}}}, \quad (6)$$

where ρ_{ma} is the density of the rock matrix which = 2.65, ρ_b is the bulk density which is determined on the log ρ_{fl} is the fluid density which = 0.74 for gas, 0.9 for oil and approximately 1.1gm/cc for water.

2.3.6. Permeability

According to Ref. [9], the permeability was calculated using the Wyllie-Rose permeability equation:

$$K = \left(\frac{250 \times \varphi^3}{S_{\text{wirr}}}\right)^2, \quad (7)$$

where K = permeability, ϕ = effective porosity and S_{wirr} = irreducible water saturation.

2.3.7. Water saturation

According to Ref. [16], the water saturation was calculated using:

$$S_w^n = \frac{a \times R_w}{R_{\text{t}} \times \phi_t^m}. \quad (8)$$

2.3.8. Modified Simandoux equation

$$\frac{1}{R_t} = \frac{S_w^2}{F \times R_{\text{w}}(1 - V_{\text{sh}})} + \frac{V_{\text{sh}} \times S_w}{R_{\text{sh}}}, \quad (9)$$

where ϕ_t, represents the formation's porosity, R_t is the true resistivity of the formation, F denotes formation factor, R_{w} is the resistivity of the water, V_{sh}, indicates the Volume of Shale, R_{sh} is the Resistivity of the Shale, S_w represents water saturation.

2.3.9. Hydrocarbon saturation

This parameter was obtained using the formula:

$$S_H = (1 - Sw), \tag{10}$$

where S_H denotes hydrocarbon saturation and Sw denotes water saturation.

2.4. 3-D seismic interpretation

Seismic interpretation was done to produce a cogent geologic narrative from a variety of seismic reflections. This entails tracing continuous reflectors across 3D data volumes on inlines and crosslines. The foundation of the geologic interpretation will then be the generated set of fault mapped, the horizon mapped and the surfaces generated.

2.4.1. Seismic to well tie

Well-to-seismic tying was carried out to assure the correctness of the interpretation of Horizon. A time-to-depth conversion curve of well 5 (Figure 7) was used for seismic-to-well tie analysis. A synthetic seismogram was produced whereby seismic reflections from seismic section were match with its corresponding converted/generated well seismic (Figure 8). A projection of Hamdex 5 well into seismic inline 5975 is shown in Figure 8. The selection/mapping of seismic occurrences (horizon to be mapped) that coincided with the tops of the reservoir sands for interpretation is the seismic to well tie that was done (Figure 9).

2.4.2. Picking of faults

Faults were identified, traced, and picked. The interpretation was done using an interval of 5 milliseconds on the inlines and crosslines. The variance attribute was utilized to enhance fault interpretation (Figure 10).

2.4.3. Horizon mapping

This is an isochronous geologic time surface that can be mapped. Three (3) horizons designated X, Y, and Z were examined as shown in Figure 11. The horizons denoted the tops of sand bodies within the Agbada Formation. The picked horizon from the seismic data was used to construct a gridded surface. A depth map of this surface was subsequently generated by applying an appropriate velocity function, which corrected structural ambiguities inherent in time structural maps. Consequently, both time and depth structural maps of the mapped horizons were developed for this study

2.5. 3-D static reservoir modelling

The characteristics of the subsurface reservoir (facies, porosity, permeability and saturation) were spatially distributed to as best possible represent the subsurface condition of "Hamphidex" field reservoirs. A cell size of $100 \times 100 \times 1$ along I, J and K were selected to capture the reservoir details considering the areal extent of the field and the thickness of the reservoir.

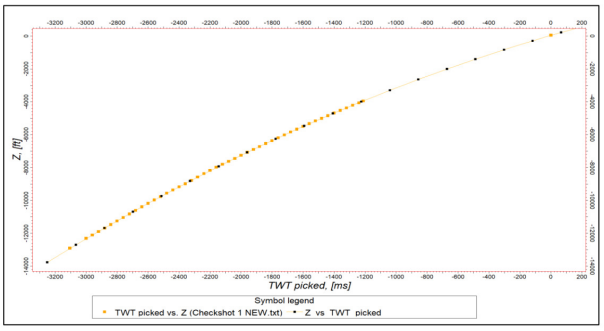

Figure 7: A time-to-depth conversion curve.

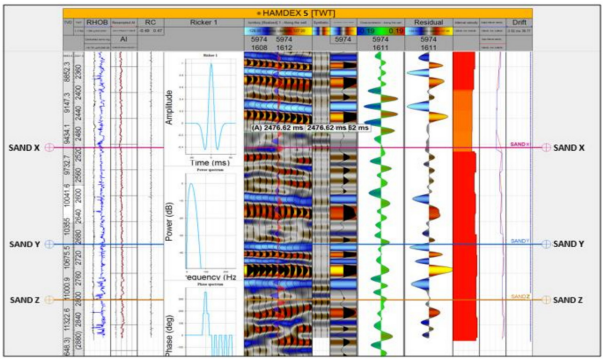

Figure 8: Synthetic seismogram between well data and seismic data

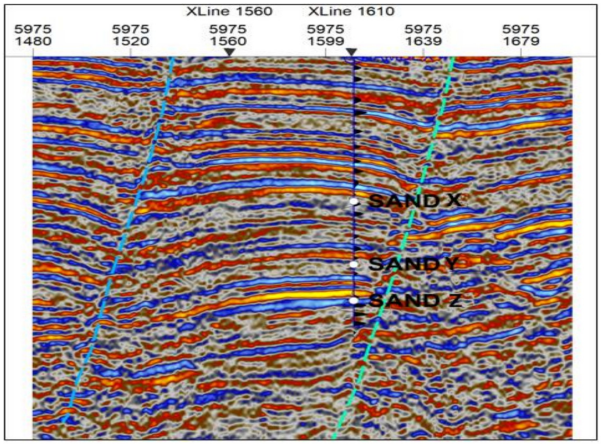

Figure 9: Seismic-to-well tie generated from well 5

2.5.1. Structural modelling

The structural model was based on the depth-converted structural maps generated from 3D seismic interpretation. The input data are depth surface maps generated from the horizons, the polygons, and the interpreted faults.

2.6. Volumetric

The Stock-Tank Oil-initially-in-place (STOIIP) was computed for all the interpreted reservoirs of interest (X, Y and Z) within the Field using the net to gross, effective porosity and

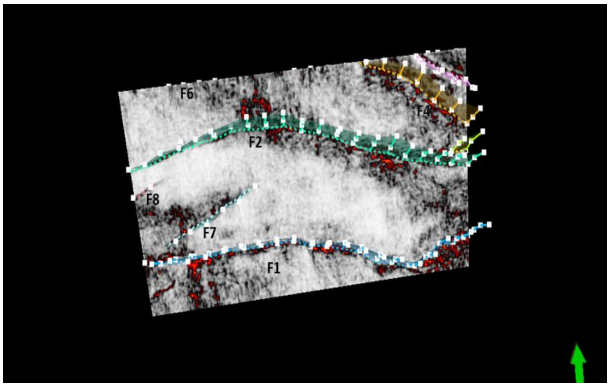

Figure 10: Variance attribute used as control for faults mapping

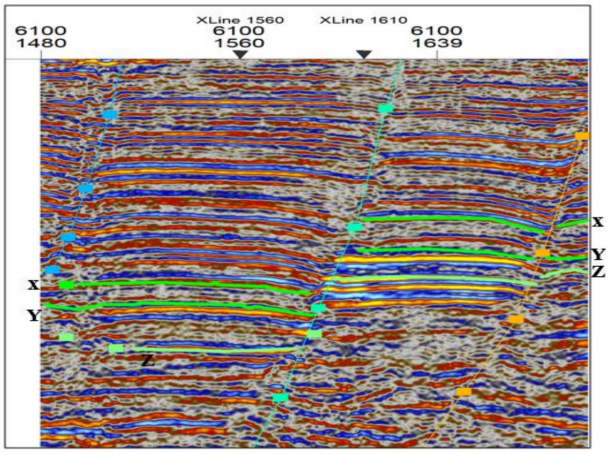

Figure 11: Horizon mapping on inline 6100.

water saturation model as input.

$$\text{STOIIP} = 7758.38 \times \text{GVR} \times \text{NTG} \times \Phi_{\text{Eff}} \times (1 - Sw) \times \frac{1}{\text{Bo}}, \quad (11)$$

where GRV=Gross Rock Volume (Area in Acres × Thickness in Feet), NTG= Net-To-Gross, ϕ_{Eff} = Effective Porosity, and Sw= Water saturation, 7758.38 = Acre-Foot to barrel conversion factor, Bo = initial oil formation volume factor, expressed in reservoir barrels per stock-tank barrel.

The Gas initially in place (GIIP) was also computed for reservoir Y within the Field using the net to gross, effective porosity and water saturation model as input.

$$\text{GIIP} = 43559.94 \times \text{GVR} \times \text{NTG} \times \Phi_{\text{Eff}} \times (1 - Sw) \times \frac{1}{\text{Bg}}, \quad (12)$$

where 43559.94 is the acre-foot to cubic-foot conversion factor.

3. Results and discussions

3.1. Well log correlation

Two distinct lithology types were identified. These are the Shale lithology and the Sand lithology. Three reservoirs that were continuous across the six (6) wells (Hamdex 02, 06, 01, 05, 04 and 07) were identified from the well log correlation done in the North-West and South-East direction. These reservoirs are Sand X, Y and Z.

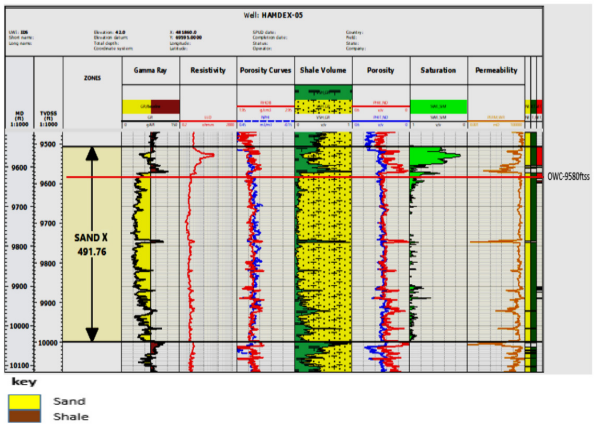

Figure 12: Logs of analysed petrophysical properties for reservoir sand X in Hamdex-05.

3.1.1. Petrophysical analysis results

Qualitative and quantitative interpretation of reservoir sand X. Reservoir Sand X was analyzed in wells Hamdex-02, Hamdex-06, and Hamdex-04, where the gross thicknesses were recorded as 505.25 ft, 582.58 ft, and 494.89 ft, respectively. These reservoirs were identified as water-bearing based on the low gamma ray log values, which are indicative of sand, coupled with low resistivity log readings. In contrast, Sand X in Hamdex-05 and Hamdex-07 (Figure 12) showed hydrocarbon-bearing potential, as indicated by high resistivity across the reservoir. In Hamdex-05, the gross thickness was 491.76 ft with a net thickness of 468.265 ft and a net pay thickness of 75.5 ft. The net-to-gross (NTG) ratio was 0.154, with an average effective porosity (Av_PHIE) of 0.267, average water saturation (Av_Sw) of 0.529, and average permeability (Av_PERM_WR) of 24,251.6 mD. Similarly, in Hamdex-07, Sand X had a gross thickness of 510.458 ft, a net thickness of 458.188 ft, and a net pay thickness of 33.144 ft. The NTG ratio was 0.065, the average effective porosity was 0.269, the water saturation was 0.489, and the permeability was 7,370.11 mD. These parameters suggest significant hydrocarbon-bearing zones in both wells. The Statistical representation of computed Petrophysical parameters using Average parameters of reservoir Sand X in Hamdex -05 & 07 is shown in Figure 13.

Qualitative and quantitative interpretation of reservoir sand Y. Reservoir Sand Y in wells Hamdex-02, Hamdex-04, and Hamdex-07 was identified as water-bearing, indicated by low resistivity log values across the sand lithology, leading to the decision not to proceed with further petrophysical analysis for these wells. In contrast, Sand Y in Hamdex-01 was hydrocarbon-bearing with a gross thickness of 376.360 ft, and detailed petrophysical analysis was conducted in Hamdex-05

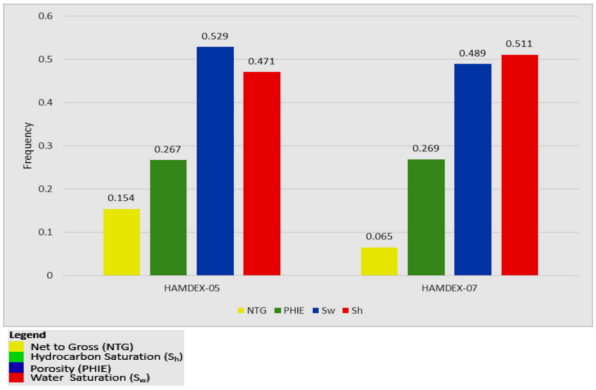

Figure 13: Statistical representation of computed petrophysical parameters using average parameters of reservoir sand X in Hamdex -05 & 07.

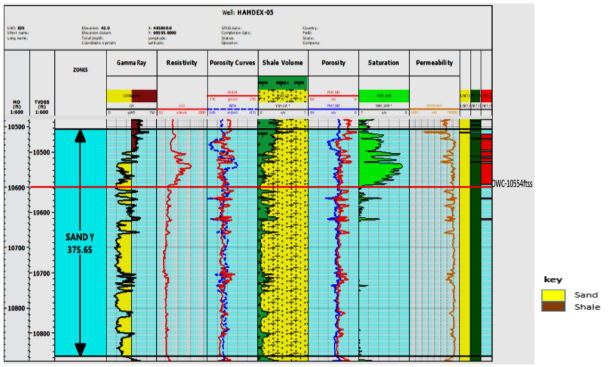

Figure 14: Logs of analysed petrophysical properties for reservoir sand Y in Hamdex- 05.

(Figure 14), where Sand Y was confirmed to be a hydrocarbon-bearing reservoir with a gross thickness of 375.654 ft, a net thickness of 335.099 ft, and a net pay thickness of 70.500 ft. The net-to-gross (NTG) ratio was 0.188, the average effective porosity (Av_PHIE) was 0.209, the average water saturation (Av_Sw) was 0.428, and the average permeability (Av_PERM_WR) was 8,218.040 mD, indicating the reservoir's significant hydrocarbon potential.

Qualitative and quantitative interpretation of reservoir sand Z. For Sand Z in wells Hamdex-06, Hamdex-05, and Hamdex-04, a quantitative petrophysical analysis was performed. In Hamdex-06 (Figure 15), Sand Z had a gross thickness of 187.781 ft, a net thickness of 100.794 ft, and a net pay thickness of 76.834 ft. The net-to-gross (NTG) ratio was 0.409, with an average effective porosity (Av_PHIE) of 0.176, an average water saturation (Av_Sw) of 0.070, and an average permeability (Av_PERM_WR) of 1017.680 mD. In Hamdex-05, Sand Z had a gross thickness of 273.203 ft, a net thickness of 219.703 ft, and a net pay thickness of 146.000 ft. The NTG ratio was 0.534, with an average effective porosity of 0.205, water saturation of 0.314, and permeability of 10618.400 mD. Similarly, in Hamdex-04, Sand Z exhibited a gross thickness of 111.191 ft, a net thickness of 62.864 ft, and a net pay thickness of 18.915 ft.

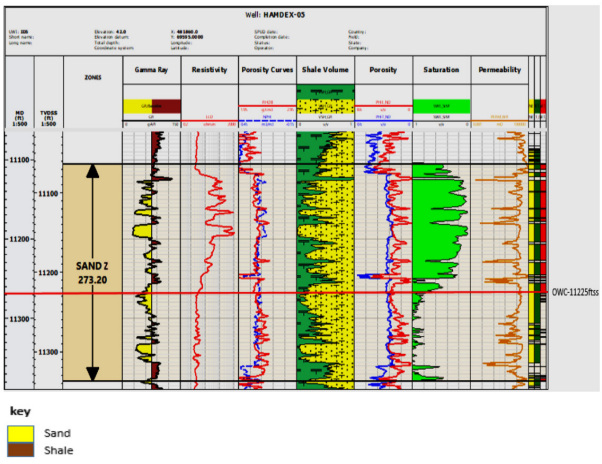

Figure 15: Logs of analysed petrophysical properties for reservoir sand Z in Hamdex- 05.

The NTG ratio was 0.170, with an average effective porosity of 0.214, water saturation of 0.251, and permeability of 2253.640 mD, indicating the reservoir's potential across these wells. A statistical representation of computed petrophysical parameters using Average parameters of reservoir Sand Z in Hamdex-05 is shown in Figure 16 and the summary of the petrophysical results from wells in "Hamphidex" field is shown in Table 1.

3.2. Structural maps

In the Sand Y Depth Map (Figure 17), two major faults, F1 and F2, are prominent and trend from the West to the East, similar to their appearance in the Sand X and Y Depth Maps. Minor faults, fault F7, and others trend from the Southwest to the Northern direction except for F4 which has East to North trend were also observed. A significant feature of the Sand Y map is a fault-assisted closure identified at a depth of approximately -10,500 ft to -10,800 ft, located about 700 ft deeper than the similar structure observed in the Sand X Depth Map. This structural closure aligns with the depths where reservoirs were delineated on the well logs, suggesting it is likely hydrocarbon-bearing. The identification of this closure is critical as it indicates potential hydrocarbon traps within the reservoir, enhancing the prospectivity of the structure for exploration. The elevation range of Sand Y's depth map highlights this feature's potential for hydrocarbon accumulation within the field.

3.3. 3-D models

The 3-D models of the facies, effective porosity (PHIE), permeability, water saturation, and contacts were generated. The top view of the models was cropped out and displayed. Also, the cross-section (x-section) which is the vertical view that cut across two wells showing the hydrocarbon concealing structure of the model was generated.

3.3.1. Facies models

The facies models for sand X, Y and Z (Figure 18) revealed two distinct facies types which are the shale and the sand facies. The sand facies is represented by the yellow colour on the

Table 1: Summary of calculated average petrophysical results from wells in "Hamphidex" field.

Wells	Gross (ft.)	Net (ft.)	NTG	PHIE (%)	PERM (mD)	Sw (%)	Sh (%)
SAND X							
Hamdex-02	502.25					WET (1)	WET (1)
Hamdex-06	582.58					WET (1)	WET (1)
Hamdex-01	474.31					WET (1)	UNDETERMINED
Hamdex-05	491.765	75.5	0.154	0.267	24251.6	0.529	0.471
Hamdex-04	474.31					WET (1)	WET (1)
Hamdex-07	510.458	33.144	0.065	0.269	7370.11	0.489	0.511
SAND Y							
Hamdex-02	427.92					WET (1)	WET (1)
Hamdex-06	SAND Y MISSING						
Hamdex-01	376.36					WET (1)	UNDETERMINED
Hamdex-05	375.654	70.5	0.188	0.209	8218.04	0.428	0.572
Hamdex-04	350.58					WET (1)	WET (1)
Hamdex-07	412.45						
SAND Z							
Hamdex-02	87.64					WET (1)	WET (1)
Hamdex-06	187.781	76.834	0.409	0.176	1017.68	0.07	0.93
Hamdex-01	128.89					WET (1)	UNDETERMINED
Hamdex-05	273.203	146	0.534	0.205	10618.4	0.314	0.686
Hamdex-04	111.191	18.915	0.17	0.214	2253.64	0.251	WET (1)
Hamdex-07	123.74						

NTG: Net-to-Gross Ratio, PHIE: Effective Porosity, PERM: Permeability in millidarcies, Sw: Water Saturation, Sh: Hydrocarbon Saturation.

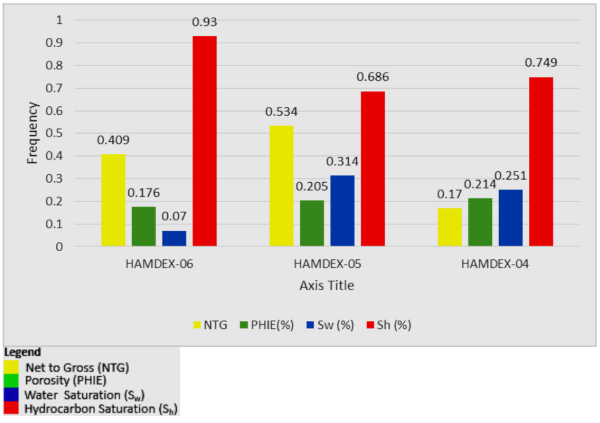

Figure 16: Statistical representation of computed petrophysical parameters using average parameters of reservoir sand Z in Hamdex-06, 05 & 04.

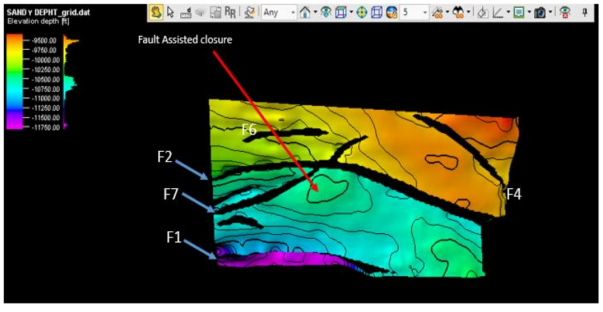

Figure 17: Sand Y depth map.

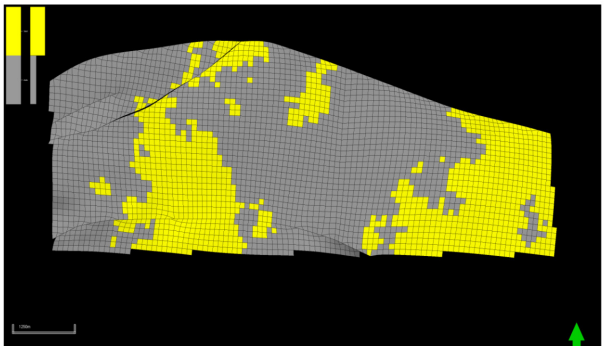

Figure 18: Sand Y facies model.

model while the shale is represented by the grey colour. The sand is more dominant as shown by the lateral model and slicing through the model in the Cross-section (Figure 19).

3.3.2. *Effective porosity models*

The effective porosity (PHIE) models of sand X, Y, and Z (Figure 20) show ranges of colours that represent various porosity ranges of the area in different directions. The light blue to green to yellow to red are areas of good to high porosity with porosity values ranging from 0.175 to above 0.30 and they are areas closer to the wells. Away from the wells are low porosity areas with colour codes ranging from purple to blue with cor-

Table 2: Volumetric for reservoir Sand X, Y, and Z.

Reservoir	GRV (acre.ft)	PV (acre.ft)	HCPV Oil (acre.ft)	HCPV Gas (acre.ft)	STOIIP (in Oil) (STB)	GIIP (in Gas) (SCF)	BO (RB/STB)	Bg (ft^3/ft^3)
X	74887	16172	12223	0	75864543		1.25	
Y	20221	4008	1380	1263	8565252	148692443801.25		0.0037
Z	106615	18592	12918	0	80178202		1.25	

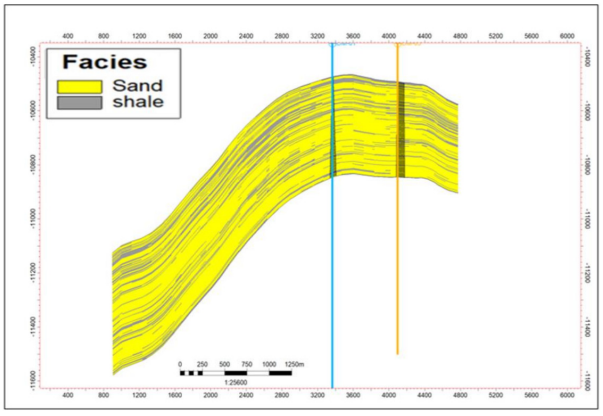

Figure 19: Sand Y facies cross-section.

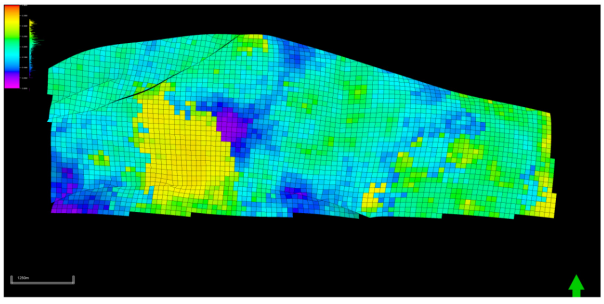

Figure 20: Sand Y PHIE model.

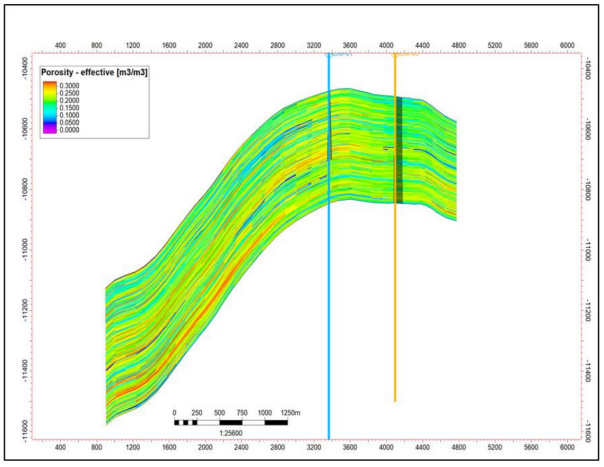

Figure 21: Sand Y PHIE cross-section.

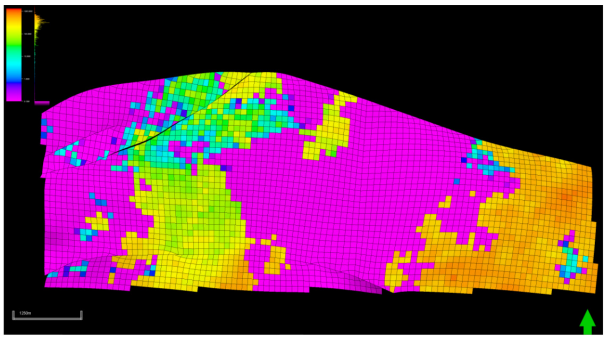

Figure 22: Sand Y permeability model.

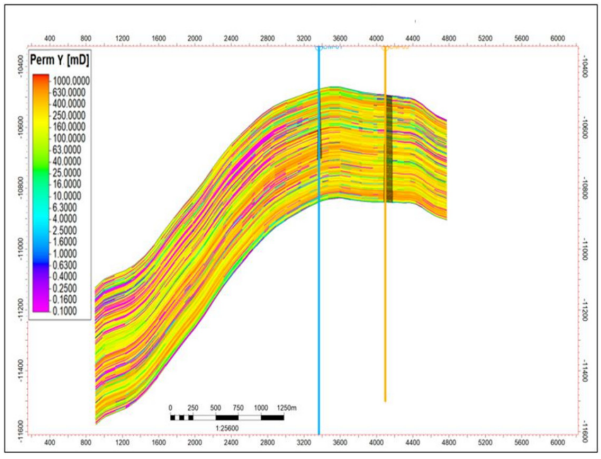

Figure 23: Sand Y permeability cross-section.

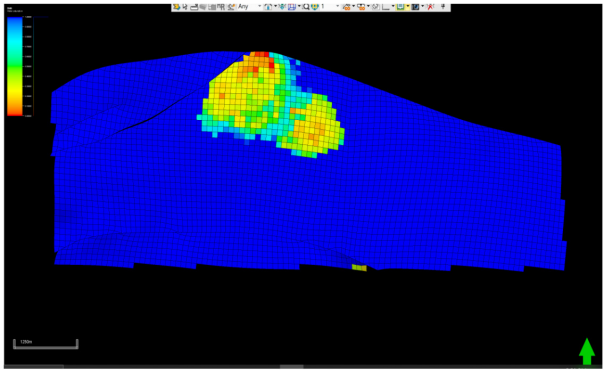

Figure 24: Sand Y Sw model.

responding values ranging from 0.075 for poor porosity areas and 0.10 to 0.15 for fair porosity areas. The cross-section (Fig-

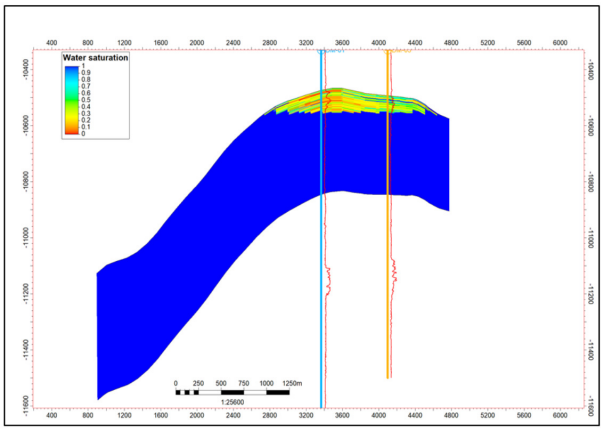

Figure 25: Sand Y Sw cross-section.

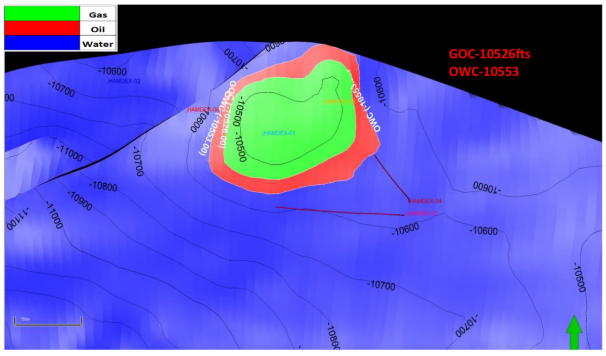

Figure 26: Sand Y contact model.

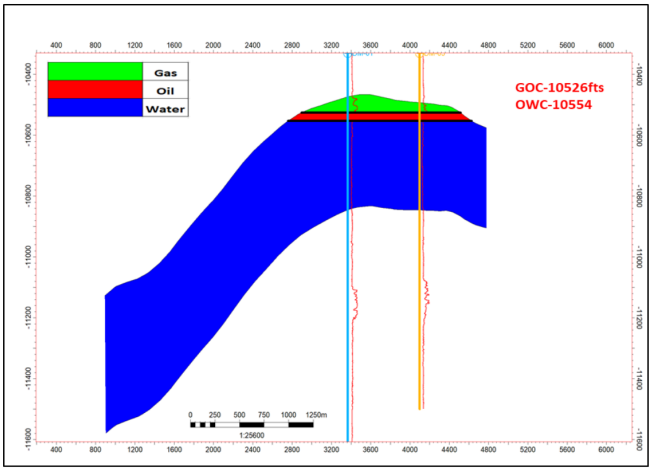

Figure 27: Sand Y contact cross-section.

ure 21) also corroborates the dominance of good to excellent porosity for the area in the model.

3.3.3. *Permeability models*

The permeability models for Sand X, Y, and Z (Figure 22) show areas with high permeability and low permeability with various colour codes ranging from purple to blue for low permeability areas/zones and light blue to green for fair permeability zone and yellow to red for high permeability zones. The corresponding value ranges from 10 mD to above 1600 mD. The Sand X, Y, and Z cross-sections (Figure 23) reveal that even though at the top of the models there are lenses of shales cutting through or slicing through the models show that permeability is good and will enable transmission of hydrocarbon during exploitation.

3.3.4. *Water saturation models*

Sand X, Y and Z water saturation models (Figure 24) show that the hydrocarbon is trapped at the peak of the structurally assisted closure which is anticlinal-like. The water-bearing zone is represented by the blue colour with the value one (1) for hundred (100) percent water saturation and the other colour represents the hydrocarbon-bearing zone with values less than one (<1) on both sand X, Y & Z, cross-section (Figure 25) and models.

3.3.5. *Contact models*

The wells were displayed on the contact models. Hydrocarbon-bearing zone was represented by green colour for gas and red colour for oil. While water zones are the blue-coloured zone in the reservoir sands models (Figure 26). Oil-water-contact (OWC) was seen at a depth of -9580ft for sand X and -10553ft for sand Y. Oil-gas-contact (OGC) was seen at -10526ft for sand Y. The resistivity logs were displayed on the cross sections (Figure 27) and it shows the hydrocarbon-bearing zones are zones with high resistivity and water-bearing zones are zones with low resistivity.

3.3.6. *Volumetric analysis*

Table 2 shows the volumetric analysis for reservoirs Sand X, Y, and Z. The Gross Rock Volume (GRV), Pore Volume (PV), Hydrocarbon Pore Volume oil (HCPV oil), and Hydrocarbon Pore Volume gas (HCPV gas) in Acre-feet respectively were determined, and the STOIIP and GIIP were calculated. Sand X STOIIP was estimated to be about 75.864 MMbbl. Sand Y has both Oil and gas. The gas was estimated to be 14.869 Bscf and the oil 8.565 MMbbl. Sand Z has an oil volume calculated to be about 80.178 MMbbl.

4. Conclusion

In this study, petrophysical analysis and 3-D modelling of reservoirs in “Hamphidex” field, using well log data and seismic data, the discrete (facies) and the continuous (petrophysical) properties of the field’s reservoir have been effectively determined. Also, the volumetric was estimated from the built 3-D models. The sand and the shale were the two distinct lithologies that were delineated. The sand lithologies represent the reservoirs. Correlation across the wells showed the continuity of reservoir sand X across the six (6) wells, reservoir sand Y across five (5) wells but missing in well (Hamdex 06), and reservoir sand Z across the six (6) wells. Reservoir sand X is prolific (it is hydrocarbon bearing in Hamdex 01, 05, and 07). Similarly, reservoir sand Y is hydrocarbon bearing in Hamdex

01 and 05. Also, reservoir sand Z has hydrocarbon in Hamdex 06, 01, 05 and 04. Other reservoirs are wet (water-bearing). The quantitative computation of petrophysical properties of the reservoir sand X, Y and Z across the wells shows the reservoir has an average effective porosity ranging from 17 to about 26 %, permeability of more than 1000 mD, and water saturation of about 7 to 50%.

The effective porosity model and its cross-sections across the reservoirs delineated in "Hamphidex" field are characterized as good to excellent porosity based on the dominant ranges of porosity values (that is 16 to above 25%) obtained from the models. Also, the dominant ranges of effective permeability values (that is 10 to above 1600 mD) obtained from the permeability models across the field showed that the field's reservoir sands are characterized as good to excellently permeable. The significance of the reservoir sands across the field having 'good to excellent' effective porosity and permeability is that the potential for holding (storability) and the potential for transmitting (transmissivity) are good. The water saturation model for sand X, Y, and Z has water saturation ranging from 35 to about 50%.

The contacts models and its cross sections and the display of resistivity log on the Cross-section in the reservoir sands show that the high resistivity zone on the logs coincides/corresponds with the hydrocarbon-bearing zones on the Cross-sections. The contact models and Cross-section show Oil-water-contact (OWC) for sand X at depth -9580 and -10553 ft for sand Y. Oil-gas-contact (OGC) was seen at -10526 ft for sand Y. Also, the computed STOIIP from all the studied reservoirs within "Hamphidex" field revealed that reservoir Sand X has about 75.864 MMbbl of oil which is the second highest in the field, while Sand Y has STOIIP of about 8.565 MMbbl and GIIP of about 14.869 Bscf. Reservoir Sand Z has the highest STOIIP of about 80.178 MMbbl.

Data availability

We do not have any research data outside the submitted manuscript file.

Acknowledgement

The authors are grateful to the Department of Geophysics, Federal University Oye Ekiti and the Nigerian Upstream Petroleum Regulatory Commission for their roles in sourcing the data for this research.

References

[1] N. Babajide, P. Arimoro & Y. Kabir, "Tax regimes of oil producing giants: a comparative study of Iran, Nigeria and United States of America", International journal of multidisciplinary research and development **2** (2015) 66. https://rgu-repository.worktribe.com/output/2344799.

[2] I. A. Oyelowo, S. A. Ayanda & O. F. Alao, "Reservoir characterization and petrophysical evaluation of a hydrocarbon reservoir in Niger Delta Basin", Journal of Petroleum Exploration and Production Technology **9** (2019) 2303. https://doi.org/10.1007/s13202-019-0651-1.

[3] A. O. Fajana, M. A. Ayuk & T. D. Omoyegun, "Comparison of modified Waxman-Smith algorithms and Archie models in prospectivity analysis of saturations in shaly-sand reservoirs: A case study of Pennay Field, Niger Delta", Earth Science Informatics **14** (2021) 1647. https://doi.org/10.1007/s12145-021-00592-8.

[4] F. Theophilus, N. Okolie & C. Chukwuma, "Petrophysical and sedimentological analysis of oil reservoirs in the Niger Delta", Petroleum Exploration Journal **38** (2021) 199.

[5] M. M. Senosy, M. Yousif & A. A. Salem, "Petrophysical and reservoir evaluation of the gas fields in the Nile Delta Basin, Egypt", Journal of African Earth Sciences **169** (2020) 103893. https://doi.org/10.1016/j.jafrearsci.2020.103893.

[6] A. O. Fajana, M. A. Ayuk & P. A. Enikanselu, "Integrated seismic interpretation and petrophysical analysis for hydrocarbon resource evaluation of Pennay-Field, Niger Delta", Journal of Petroleum Exploration and Production Technology **9** (2019) 123. https://doi.org/10.1007/s13202-018-0579-4.

[7] A. O. Fajana, "Hydrocarbon reservoir characterization methodologies and uncertainties as a function of spatial location: a review from gigascale to nanoscale", FUOYE Journal of Pure and Applied Sciences (FJPAS) **8** (2023) 82. https://fjpas.fuoye.edu.ng/index.php/fjpas/article/view/276.

[8] A. O. Fajana, "3-D static modeling of lateral heterogeneity using geostatistics and artificial neural networks in reservoir characterization of 'P' Field, Niger Delta", NRIAG Journal of Astronomy and Geophysics **9** (2023) 178. https://doi.org/10.1080/20909977.2020.1727674.

[9] G. Asquith & D. Krygowski, *Basic well log analysis*, Vol. 16, American Association of Petroleum Geologists, Tulsa, 2004, pp. 31-34. https://doi.org/10.1306/Mth16823.

[10] Google Earth, 2023, "Study area delineated using Google Earth imagery", Nigeria. N4°37'40" and N4°37'40" to E6°48'20" and E 6°47'20". [Online]. https://www.google.com/earth/.

[11] NIMET, 2024, Warri station annual average precipitation and rainy days, period 2022-2024. [Online]. https://nimet.gov.ng/datarequest.

[12] P. Stacher, "Present understanding of the Niger Delta hydrocarbon habitat", in *Geology of Deltas*, M. N. Oti & G. Postma (Eds.), A. A. Balkema, Rotterdam, 1995, pp. 257-267. https://www.researchgate.net/publication/281508240_Present_understanding_of_the_Niger_Delta_hydrocarbon_habitat.

[13] W. L. M. Tuttle, R. R. Charpentier & M. E. Brownfield, "The Niger Delta petroleum system: Niger Delta province, Nigeria, Cameroon and Equatorial Guinea, Africa", USGS. Denver Colorado. Open-file report 99-50-H, 1999. [Online]. https://doi.org/10.3133/ofr9950H.

[14] T. J. A. Reijers, S. W. Petters & C. S. Nwajide, "The Niger Delta Basin", in *African Basins--Sedimentary Basin of the World 3*, R. C. Selley (Ed.), Amsterdam, Elsevier Science, 1997, pp. 151-172. https://doi.org/10.1016/S1874-5997(97)80010-X.

[15] H. Doust & E. Omatsola, "Niger Delta", in *Divergent/passive margin basins*, J. D. Edwards & P. A. Santogrossi (Eds.), AAPG Memoir 48: Tulsa, American Association of Petroleum Geologists, 1989, pp. 239-248. https://doi.org/10.1306/M48508C4.

[16] G. E. Archie, "The electrical resistivity log as an aid in determining some reservoir characteristics", Petroleum Transactions of AIME **146** (1942) 54. https://doi.org/10.2118/942054-G.